UNIVERSITY OF CALIFORNIA, SAN DIEGO

Characterization and Application of a Long Term Noncytotoxic Live Cell Labeling Probe

A thesis submitted in partial satisfaction of the requirements for the degree

Master of Science

in

Bioengineering

by

Jieying Li

Committee in charge:

Professor Shu Chien, Chair
Professor Ju Chen
Professor Sheng Zhong

2013

The thesis of Jieying Li is approved and it is acceptable in quality and form for publication on microfilm or electronically:

_____

_____

_____

Chair

University of California, San Diego

2013

TABLE OF CONTENTS

LIST OF FIGURES

ACKNOWLEDGEMENTS

I would like to acknowledge my P.I. Dr. Shu Chien for his gracious guidance and support, and my mentor Dr. Dayu Teng for the extensive training and invaluable advices. I am grateful to my fellow labmates, Michael Liu, Kevin Shih, Andy Parsy and Lu Yang, for their contributions to my research. I would also like to thank my committee members Dr. Ju Chen and Dr. Sheng Zhong.

ABSTRACT OF THE THESIS

Characterization and Application of a Long Term Noncytotoxic Live Cell Labeling Probe

by

Jieying Li

Master of Science in Bioengineering

University of California, San Diego, 2013

Professor Shu Chien, Chair

Fluorescent molecular probes for cell labeling are useful in visualizing and quantifying cells. Many commercially available probes are cytotoxic and not ideal for multi-day live-cell tracking. In order to assess their effects on cell proliferation, the number of cells exposed to a probe was automatically counted every day for five days using an image analysis software called CellProfiler. MitoTracker Red at 62.5 nM showed the least interference with cell growth and produced desirable signals and hence

was identified as the most suitable live-cell staining agent for long-term tracking. MitoTracker Red was subsequently used to quantify the effects of honokiol, an extract from a plant, on vascular cell proliferation. Preliminary finding suggested a nontoxic concentration of 55-60 μM for BAECs and BSMCs that could inhibit cell proliferation. This result may serve as the first step in assessing the use of honokiol in drug-eluting stents. MitoTracker Red was also applied to monitor the real-time effects of thrombectomy devices in live-cell artificial vessels. Four clot retrieval devices for stroke, Separator 3D, Trevo Pro Retrival System, Solitaire and Merci were separately tested in the artificial vessels lined with live endothelial cells that were developed for this study. The degrees of damages induced by the devices were revealed by MitoTracker Red staining. The results validated the application of live-cell artificial vessels in the study of endovascular devices. This thesis work identified MitoTracker Red as the most suitable multi-day live-cell tracking agent among several. Its applications then produced meaningful results in assessing the effects of drugs and thrombectomy devices.

CHAPTER ONE

Identification of a Long Term Noncytotoxic Live Cell Labeling Probe

Introduction

Quantification of cell number is a simple but critical process in assessing cell growth, which is usually used as a criterion in evaluating cellular response to external stimuli such as mechanical forces and drug-like molecules. During drug screening, it is often important to evaluate the long-term effect of the drug on cell growth. Even with a surgical procedure conducted in an in vitro model, where the immediate cellular and tissue response is the main concern, the long-term systematic impact may not be obvious until sometime after the procedure. Therefore, it is crucial to have a method to track the cell number over an extended period of time.

Staining cellular structures with fluorescent tags is a widely used technique in microscopy for visualizing subcellular organelles, examining tissue structures, as well as quantifying cell number. One prevalent method that has been used for decades is immunofluorescent staining, which uses fluorophore tagged antibodies to target specific biomolecules within a cell. However, since the cell membrane is impermeable to antibodies, unless the protein of interest is located on the cell membrane or in the extracellular space, immunofluorescent staining can only be applied to fixed cells [1].

Fluorescent protein is a powerful tool for long-term cell tracking as the cells produce stable internal fluorephores [2]. However, since genetic manipulation is required to incorporate the fluorescent gene into the cell genome, it is not suitable for studying primary cells. Fluorescent proteins are great for tracking genetic expression and protein localization, but if quantifying the cell number is the major goal, establishing a

fluorescent cell line for each cell type of interest can be too time consuming and not cost effective.

There is a wide range of fluorophores that can be used in live cell staining. These fluorescent probes target different subcellular organelles and come in a variety of colors. However, not all of them are suitable for long-term tracking usage. Nucleic acid probes such as DAPI and Hoechst are very potent nucleus dyes that are widely used. The mechanism of interaction between Hoechst and DNA has been well studied, including the effect of dye concentration, ionic strength and pH on fluorescent intensity and sensitivity [3, 4]. Although live cells can be stained with these probes, since the DNA is modified, cells are generally nonviable afterwards.

Nonetheless, there are a number of fluorescent probes that have shown to be non-cytotoxic, including alamar Blue, MitoTracker, LysoTracker, calcein AM and vybrant cell labeling reagent.

Alamar Blue is a resazurin that fluoresce when reduced to resorufin, which is localized to the nucleus when cells are dead but remain in the cytoplasm when cells are alive [5]. It has been used in high-throughput screening assays to select in vitro cytotoxic drugs [6]. However, alamar Blue has been shown to accumulate in the medium and interfere with the cellular signal, in addition, it can be readily reduced to a non-fluorescent product in metabolic active cells and results in signal reduction [5].

MitoTracker probes are chloromethyl-X-rosamines that label the mitochondria through the thiol reactive chloromethyl groups [7]. It is non-cytotoxic in the concentration range of 100-250 nM and can be used in confocal microscopy and flow

cytometry [8]. Apart from cell labeling, it has been used to study mitochondrial membrane potentials and apoptotic pathways [9, 10].

Lysotracker is a lysosomal marker working at nanomolar concentrations [11]. It is membrane permeable at neural pH but prefers acidic compartments due to its basic amine on the multi-pyrrole ring structure, and it can be used in protein localization and cell labeling with confocal microscopy [12].

Calcein AM is a cytoplasmic fluorescent dye that enters the cell as a non-fluorescent calcein-acetoxymethylester, and fluorescent when converted into calcein by intracellular esterases [13]. It has been used in microplate assays, real-time imaging and oxidative activity study in live cells [13, 14].

Vybrant DiO/DiL/DiD are carbocyanine dyes that function as plasma membrane markers by binding to phospholipids [15]. They have been used to study plasma membrane organization in living cells by laser scanning microscopy [16].

Each of the staining reagents mentioned above has been used individually in different live cell studies for various purposes. However, there has not been a systematic study to compare all these reagents and assess their efficacy towards cell viability and long-term tracking. In this paper, I focus on the commercially available cell labeling reagents and screen for the ones that are non-cytotoxic and suitable for long-term cell number quantification study.

Methods

Signal Strength Assay

U87 glioblastoma cells were cultured to near confluency in DMEM (Gibco by Life Technologiess) with 10% FBS (Omega Scientific) and then seeded to 80% confluency in 96-well plates. LysoTracker Red (600 nM, 60 nM, 6 nM), MitoTracker Red (2.5 μM, 250 nM, 25 nM), MitoTracker Green (2.5 μM, 250 nM, 25 nM), alamarBlue (1X, 2X), calcein AM (50 μM, 5 μM, 500 nM), Vybrant DiO (2 nM, 5 nM, 25 nM), DiD (2 nM, 5 nM, 25 nM) and DiL (2 nM, 5 nM, 25 nM) (all from Invitrogen by Life Technologies) were added to the corresponding wells, incubated for 30 min, and replaced with growth medium. Cells were viewed under a fluorescence microscope (Nikon Diaphot 300) at 10X magnification with an excitation wavelength of 405nm (UV), 488 nm (blue) or 532 nm (green).

The concentration ranges for MitoTracker Red and calcein AM were narrowed down to 25 - 250 nM and 0.25 – 5 μM, respectively, for further testing.

Cell Viability Assay

Bovine artery endothelial cells (BAEC) were cultured to near confluency in DMEM with 10% FBS and then seeded to 5% confluency in 96-well plates on day 0. Starting on day 1, cells in their corresponding wells were stained everyday with 62.5 or 125 nM for MitoTracker Red and 250, 500 or 1000 nM for calcein AM for 30 min, and replaced with growth medium. Three repeats were used for each condition. Twelve consecutive images were taken for each well at 4X magnification to capture the entire well at each time point. The cell growth in each well was tracked for 5 days. As a

comparison, 5 μg/ml Hoechst (Invitrogen by Life Technologies) was used to stain a fresh set of cells at each time point (all seeded on day 0).

Image Analysis

A Matlab program was used to generate a composite image of each well by combining the 12 images. Each composite image was processed with a six-step CellProfiler pipeline to obtain the cell count. The circular well part of each image was first cropped out and the intensity of the image was rescaled. A background illumination function was calculated and subtracted from the image to correct for uneven background. After the cell feature was enhanced in gray scale, the cells were identified from the image with the object size set between 2 and 25 pixels, and objects outside the size range were discarded. The thresholding method used was background adaptive with a threshold correction factor set between 1.0 and 1.5. The lower and upper bounds of the threshold were adjusted for each set of images in the range of 0.01 to 1. To distinguish individual cells aggregated in clumps, the size of the smoothing filter was set to 1 and the object intensity instead of shape was chosen as the main criteria to distinguish and draw dividing lines between clumped objects.

Results

The following staining reagents were tested for signal strength with U87 glioblastoma cells: MitoTracker Red/Green, calcein AM, LysoTracker Red, alamarBlue and Vybrant DiO/DiD/DiL. Figure 1 shows the poor signal strength produced by

MitoTracker Green, LysoTracker Red, alamarBlue and Vybrant DiO/DiD/DiL under the upper limit of their respective recommended working concentrations.

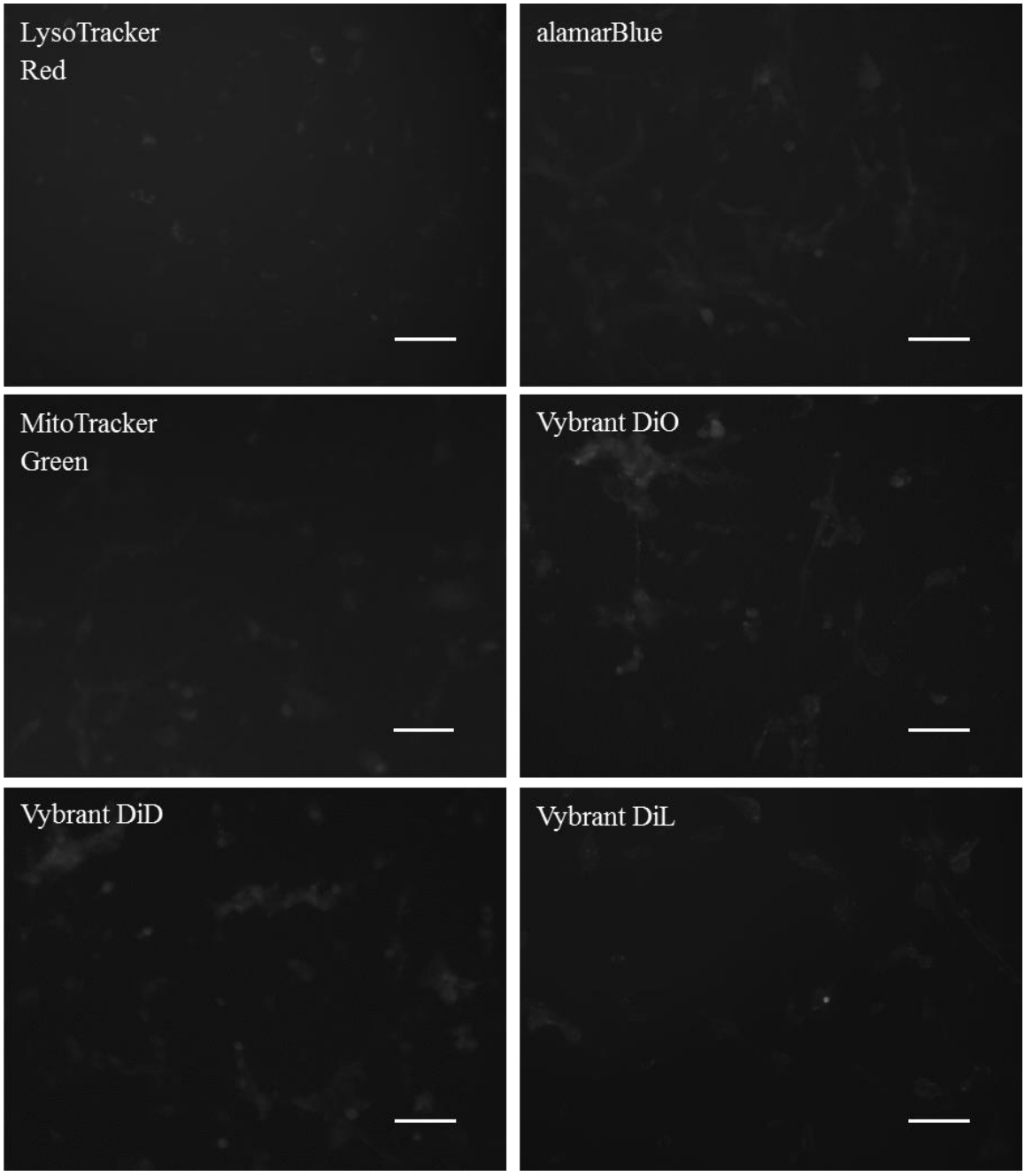

Figure 1. U87 cells stained with Lysotracker Red, alamarBlue, MitoTracker Green, Vybrant DiO/DiD/DiL. Scale bar = 100 μm.

On the other hand, MitoTracker Red and calcein AM gave discernable signals within their working concentrations, as shown in figure 2.

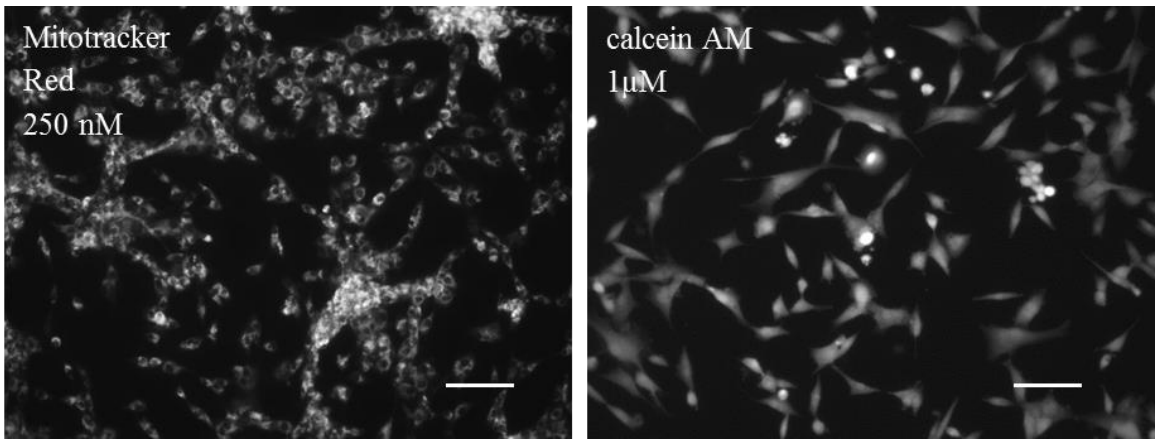

Figure 2. U87 cells stained with MitoTracker Red and calcein AM, with working concentration of 25-500 nM and 1-10 μM, respectively. Scale bar = 100 μm.

Based on the signal strength, the eight staining reagents tested were narrowed down to MitoTracker Red and calcein AM. To determine whether they were suitable for long-term cell tracking, these two reagents were then tested for their effects on cell proliferation under different staining concentrations. Bovine artery endothelial cells (BAEC) were grown in 96-well plate and stained with different concentrations of MitoTracker Red and calcein AM. Each well was stained with the same reagent condition everyday and the cell proliferation in each well was tracked for a 5-day period. The cell growth under these staining conditions was compared with that with Hoechst dye. Since Hoechst targets the cell nucleus and makes cells non-viable after the staining, instead of tracking cells in each well with Hoescht over time, a fresh set of wells were stained with Hoeschst at each time point to monitor the cell growth without any prior chemical treatment.

To quantify the number of cells in each well without bias, a composite image of each well was generated by stitching together 12 separate exposures in Matlab (figure 3). The composite images were then processed with CellProfiler through several steps to obtain the cell count in each well. A typical pipeline of CellProfiler and the corresponding output of each step is shown in figure 4. First, the circular well was cropped out from the original image to eliminate the excess background signal outside the well (figure 4a). Then, the contrast of the cropped image was enhanced by rescaling the intensity (figure 4b). Next, the uneven background noise within the well was further reduced using the correct illumination function (figure 4c). To facilitate cell identification, the cells were viewed as long and thin neurites and their outlines were enhanced (figure 4d). Finally, the cells in the processed image were identified and counted after setting the selection criteria including threshold level, effective cell size, and smoothing filter value. The output from the CellProfiler is shown in figure 5.

The specific pipeline of CellProfiler was adjusted for each stainging condition due to different image intensity and background noise. BAECs stained with different staining conditions are shown in figure 6. The effect of each staining reagent on cell proliferation is compared in figure 7, where the cell count was normalized to the initial seeding density for each condition. MitoTracker Red 62.5 nM was the only condition that did not significantly affect the cell growth compared to Hoechst.

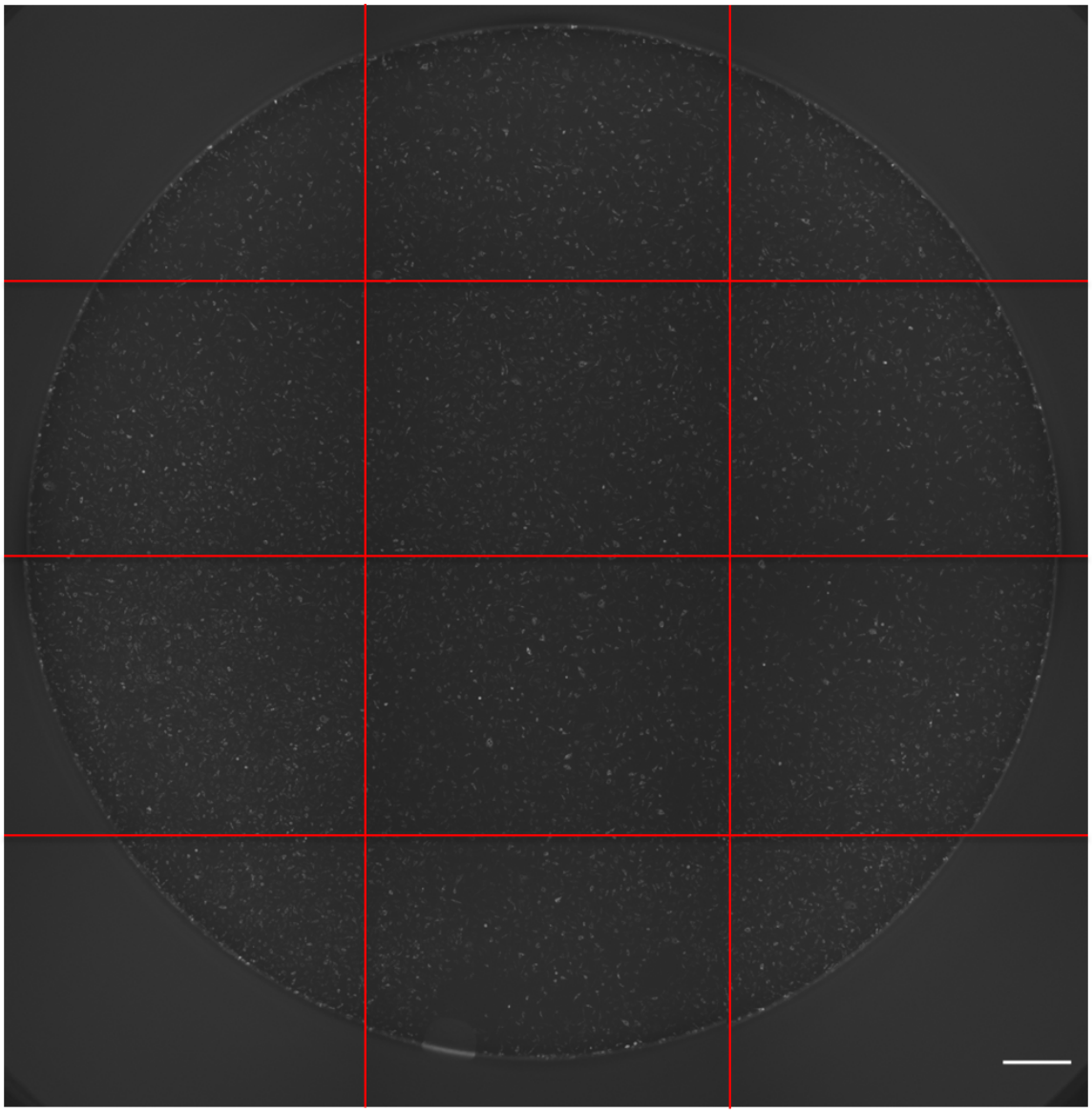

Figure 3. A composite image of a well generated by combining 12 individual images. BAECs stained with 62.5 nM of MitoTracker Red. Scale bar = 400 μm.

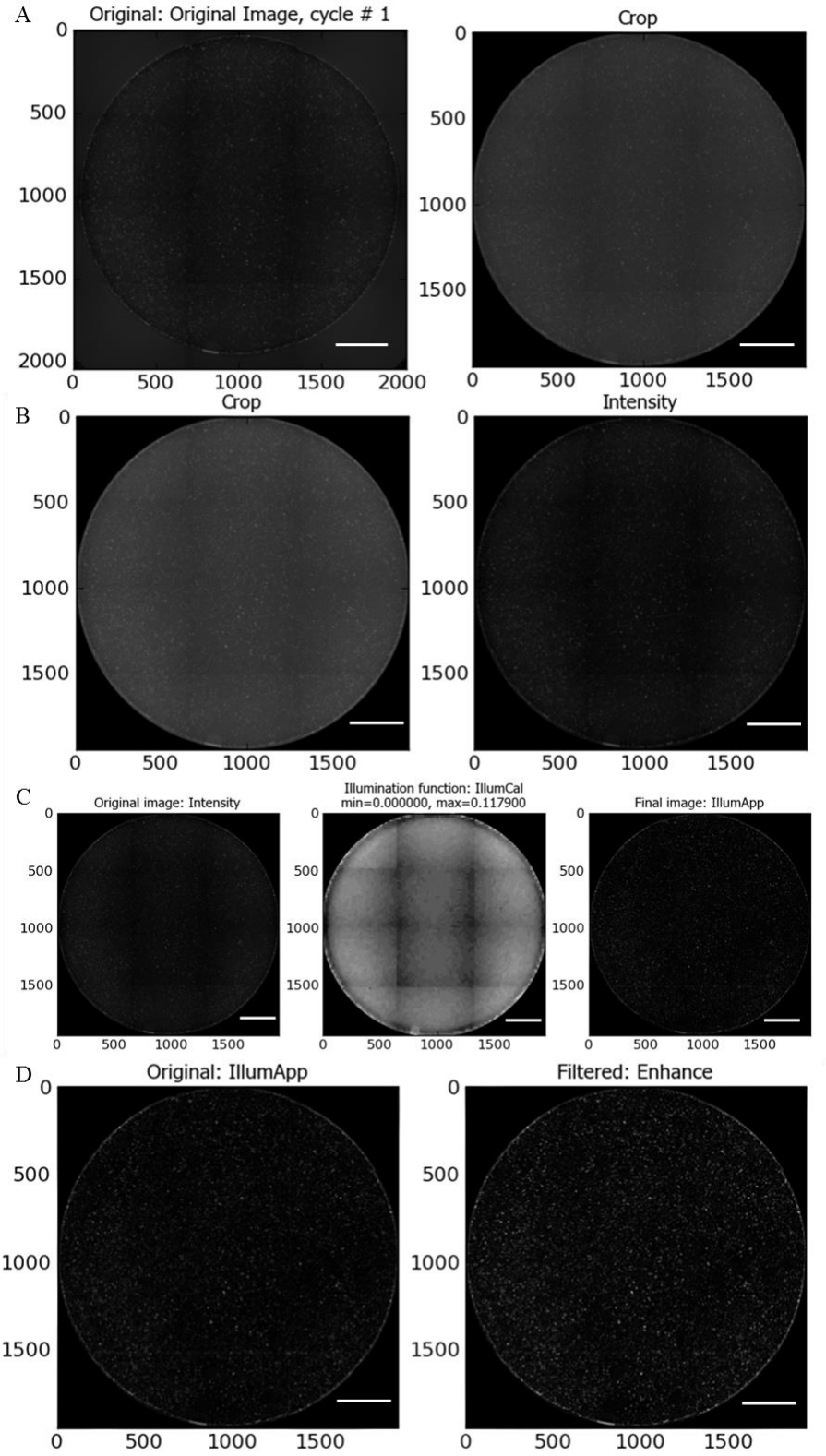

Figure 4. Imaging processing pipeline of CellProfiler. A: crop image. B: rescale intensity. C: correct illumination. D: enhance cell outline. Scale bar = 1 mm.

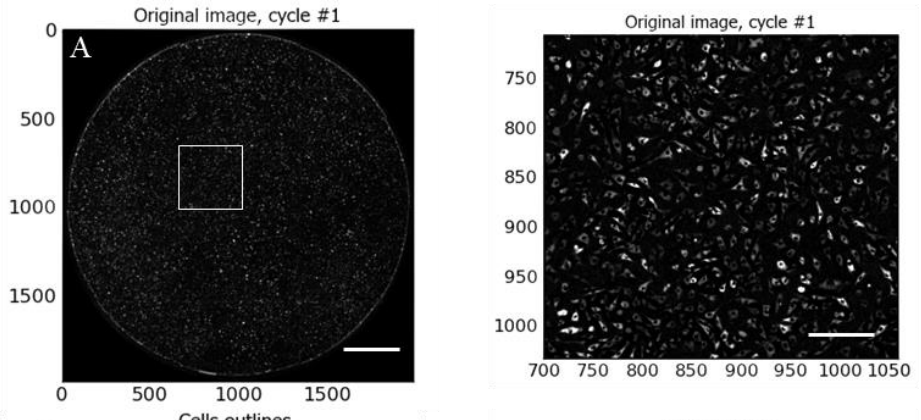

Threshold	0.038
# of identified objects	14194
10th pctile diameter	2.8 pixels
90th pctile diameter	9.8 pixels
Area covered by objects	13.1 %
Smoothing filter size	1.0
Maxima suppression size	1.3

Figure 5. Output of CellProfiler. A: original image. B: identified objects, with green outline indicating accepted objects that meets all selection criteria and red outline showing discarded objects based on size. C: identified objects with primary colors for ease of distinguishing. The region enclosed by the white square is enlarged on the right side.The table at the bottom summarizes the information extracted from the original image. Scale bar = 1mm (left), 200 μm (right).

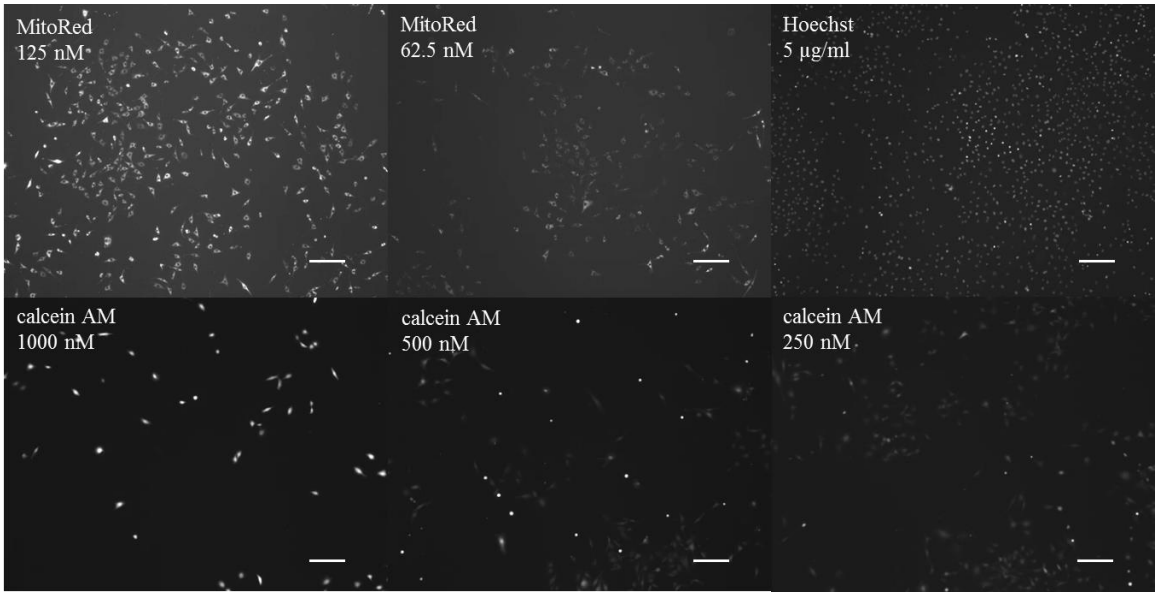

Figure 6. BAECs stained with different staining conditions. Scale bar = 200 µm.

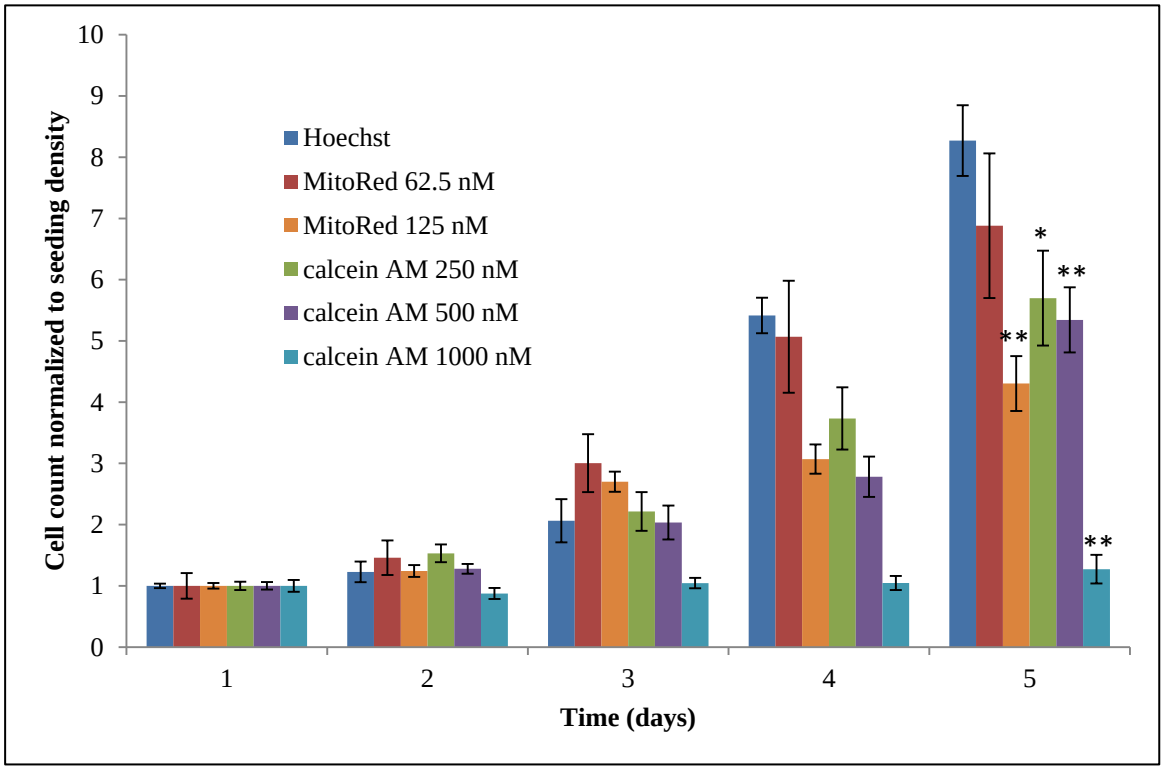

Figure 7. Effects of MitoTracker Red and calcein AM on cell proliferation. Cell counts were normalized to the initial seeding density. N=3, error bars represent SEM.
*: $p<0.05$**: $p<0.01$ compared to Hoechst.

Discussion

In this study, the eight live-cell tracking agents were assessed for multi-day cell quantification application. The goal was to identify the ones that would provide good fluorescent signals for imaging analysis but not interfere with cell proliferation. Among the eight tested, MitoTracker Green, LysoTracker Red, alamarBlue and Vybrant DiO/DiD/DiL generated much less fluorescent intensity under our experimental conditions (Figure 1), while MitoTracker Red and Calcein AM provided bright fluorescent signals (Figure 2). Because of these initial results, the efforts had been primarily focused on validating the efficacy of MitoTracker Red and Calcein AM in multi-day live-cell tracking. The most important criterion of this efficacy was how inert the agents were to cell proliferation.

One of the most direct methods to assess the cell proliferation was to quantify and compare the increment in the number of cells exposed to the tracking agent and the control condition. In this study, the whole well of 96-well plate was scanned to construct the composite image of the cells in an entire well. Compared to sampling images in a well, the whole-well scanning avoids sampling inconsistencies. However, the large number of cells in the composite image of a whole well made it impossible to manually count. To automate the cell counting process, CellProfiler, a very powerful imaging analysis software was used. The program has series of functions called “pipeline” that can effectively eliminate most background noise, enhancing cell features and determine the boarders of cells through built-in pattern recognitions. Numerous pieces of information can be outputted, such as cell area, location, distribution and cell count. However, the parameters of each function needed to be adjusted specifically for every set

of images to accurately capture the information. The most sensitive criteria include average cell size, threshold level, and smoothing filter. Objects outside the size range were discarded; the threshold set the cutoff line between background noises and object signal; and the smoothing filter determined the degree to which objects were grouped. Minor change in these parameter values greatly altered the object identification readout. So far, there is no systematical way to optimize these parameters. The pipeline functions used to obtain the cell count for each batch of images were manually adjusted based on trial-and-error and visual confirmation. However, the error associated with the cell count was difficult to quantify, and hence was not included in the results. Since the pipeline used for each experimental condition was consistent, the growth trend for each staining condition was reliable. Because the difference in image quality among different staining conditions was taken into account in batch specific pipelines, the comparison drawn between different conditions was acceptable as well.

Figure 7 indicates that MitoTracker Red 62.5 nM (within the working concentration range of 25-500 nM) was the only condition that did not significantly affect cell growth, as all the other conditions were statistically different from Hoechst at day 5. All the concentrations tested for calcein AM inhibited cell growth to various degrees. Although it was possible to pursue even lower concentrations, since the highest concentration used (1000 nM) was already at the lower boundary of the suggested working concentration range (1-10 μM), there is sufficient evidence to suggest that calcein AM is not a suitable live cell tracking reagent in our experimental setting.

CHARPTER TWO

Application of the Live Cell Labeling Probe: Honokiol Drug Test

Introduction

Herbs have been extensively used in traditional Chinese and Japanese medicine for treating various diseases, while Western medicine has extracted the active ingredients from these herbs and identified the mechanism of action for some. Honokiol and magnolol, isomeric of each other, are two active components extracted from the bark and seed cone of Magnolia obovata, which is used in traditional Japanese medicine Houpo and saiboku-tu [17, 18].

There is evidence that honokiol and magnolol have anti-tumor, anti-inflammatory and anti-microbial properties. The anti-tumor activity of honokiol has been shown for a variety of tumors in vitro, including myeloma cells, colon cancer cells and breast cancer cells, and honokiol was more effective towards angiosarcoma cells than magnolol [19-21]. The anti-inflammatory effect of honokiol was shown in a mouse model of autoimmune disease by retarding the progression of collagen-induced arthritis [22]. Honokiol and magnolol could also inhibit the growth of periodontal pathogens, although less potent than tetracycline [23].

In addition, honokiol and magnolol exhibit the potential as anti-thrombotic agents. The angioplasty-induced vascular endothelial wall damage often leads to the outgrowth of vascular smooth muscle cells (VSMC) and eventually results in restenosis [Ref?]. Antioxidants have been used to coat the stent in preventing restenosis. Magnolol has been shown to induce apoptosis of VSMC and limit the percentage of cells that entered the S phase [24, 25], while honokiol inhibited DNA synthesis of VSMC and caused G1 cell

cycle arrest [26]. The anti-proliferative effect of honokiol towards SVR endothelial cells has been shown to be associated with TNFα-related apoptosis pathway [19]. However, it also has been found to have protective effect towards rat SMC against oxidized low density lipoprotein injury, suggesting its potency as a thrombosis inhibitor [27].

The anti-thrombotic property of honokiol in addition to its versatile nature makes it a good candidate for thrombosis treatment. Most studies carried out so far, however, obtained the cell count within 24 hour of treatment [24-26], thus do not address the long-term effect of honokiol on the cells. In this study, I aimed to treat both vascular smooth muscle and endothelial cells with honokiol over an extended period of time. MitoTracker Red, the live cell labeling reagent identified in the previous chapter, is used to track and quantify the cell number over the time course to determine the optimal concentration of honokiol in inhibiting cell proliferation.

Methods

Both bovine artery endothedial cells (BAEC) and bovine smooth muscle cells (BSMC) were cultured with 10% FBS in DMEM to near confluency and seeded at 5% confluency in 96-well plates. Cells were allowed to attach and spread overnight before treatment with honokiol (Dr. Jack Arbiser, Emory University). The honokiol concentrations used for the first round were 5, 50 and 100 μM, second round 40, 60, 80 and 100 μM, and third round 45, 50, 55, 60 and 65 μM, with three repeats for each condition. 2% DMSO (ATCC) was used as the control. At each time point, cells were stained with 62.5 nM MitoTracker Red for 30 min, replaced with a growth medium

containing honokiol and imaged with a fluorescent microscope (532 nm excitation, Nikon Diaphot 300). CellProfiler was used for image analysis as described previously.

Results

Honokiol has been reported to have an IC_{50} of 61.6 µM against the growth of human U251 glioma cells [28]. To screen for the growth inhibition concentration of honokiol against BAEC and BSMC, the preliminary concentration range for testing was chosen to be 5 – 100 µM (figure 8). This range was narrowed down to 40 – 100 µM to determine the plateau in the growth curve (figure 9). During the third round of testing, the range was further narrowed down to 45 – 65 µM and the duration of the study was extended (figure 10). MitoTracker Red, identified in the previous chapter, was used to stain the cells for imaging at 62.5 nM. Cell counts were obtained with CellProfilier, as described before. Morphological changes of the cells, in addition to cell lost, under different honokiol concentration were also observed, as illustrated in figure 11.

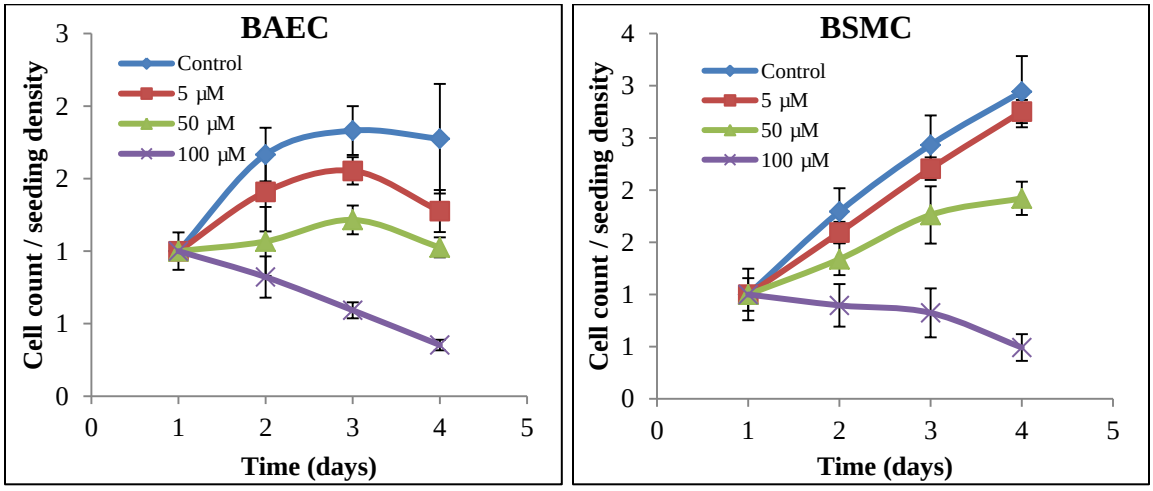

Figure 8. First round of honokiol test. Concentration range: 5 – 100 µM. N=3, error bars represent SEM.

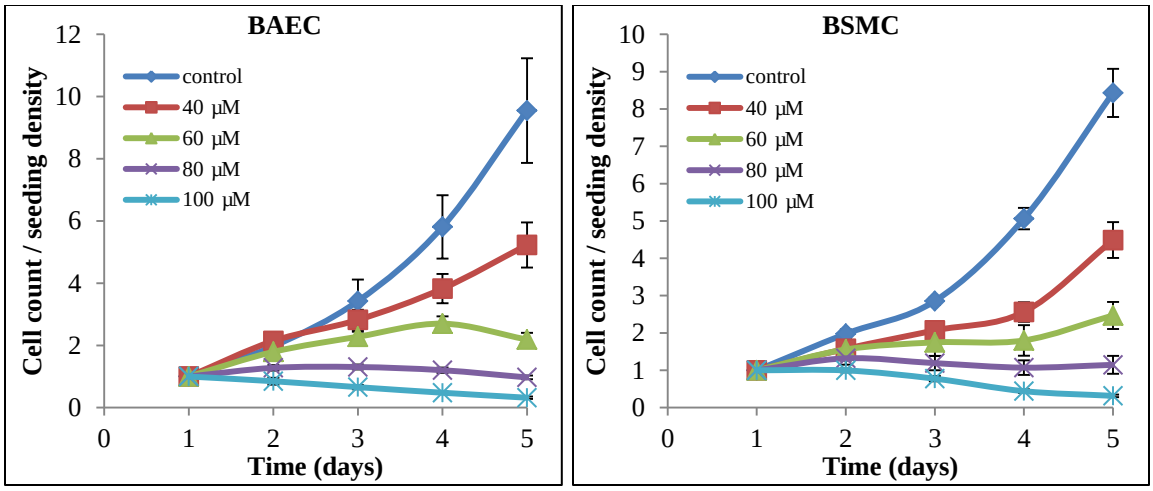

Figure 9. Second round of honokiol test. Concentration range: 40 – 100 µM. N=3, error bars represent SEM.

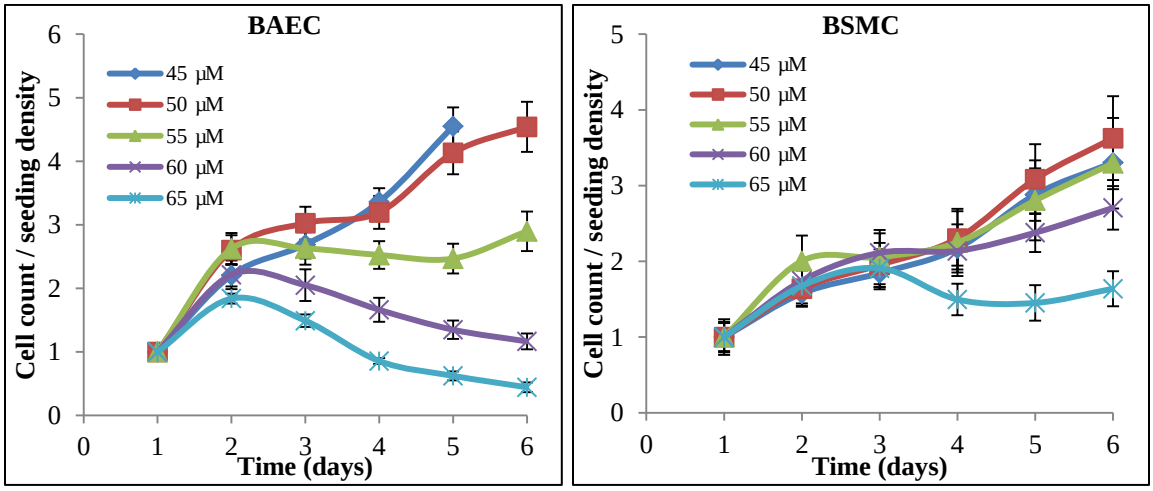

Figure 10. Third round of honokiol test. Concentration range: 45 – 65 µM. N=3, error bars represent SEM.

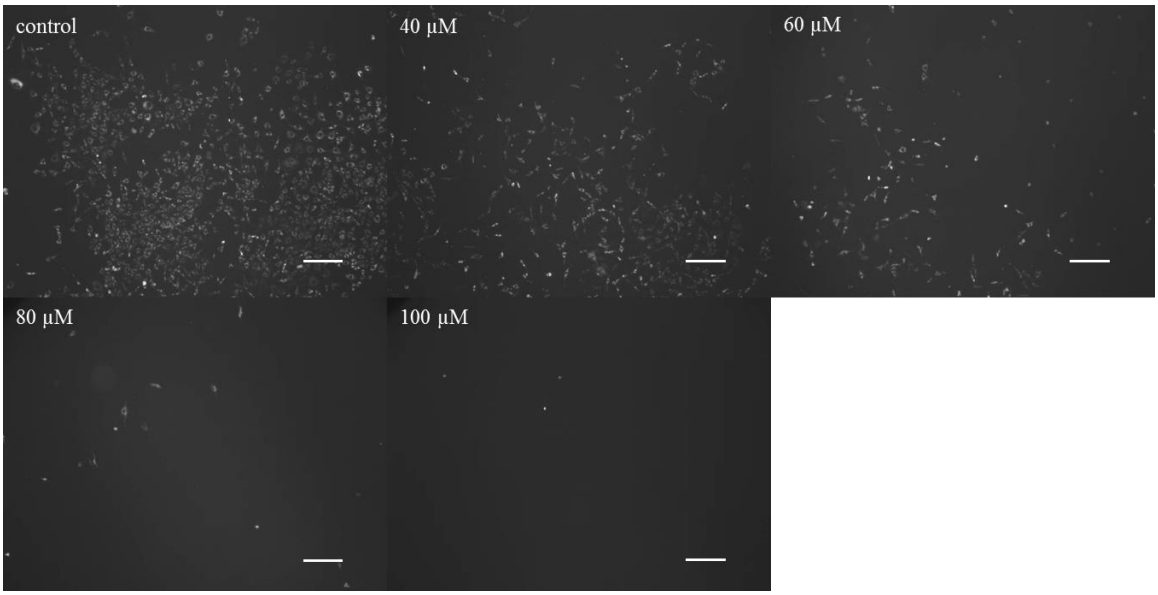

Figure 11. BAECs under different concentrations of honokiol on day 5. Cells stained with MitoTracker Red. Scale bar = 200 µm.

Discussion

The drug-eluting stent was designed to reduce re-stenosis after angioplasty by slowing down the proliferation of surrounding smooth muscle cells. In this study, the effect of honokiol on vascular cells was assessed as the first step in exploring the potential of honokiol to be applied in drug-eluting stents. Because of the consistency of the signal quality and its minimal interference with cell growth, MitoTracker Red was chosen to quantify the effect of honokiol on vascular cells.

The growth of both BAEC and BSMC was inhibited by honokiol in a concentration-dependent manner. The effect of honokiol on these cells was first tested at 5, 50 and 100 µM (Figure 8). The drug-eluting stent was designed to slow down the vascular cell proliferation, the desirable concentration needed to prevent the number of cells from increasing but not reducing the number. Thus, the concentrations near 50 µM (45 – 65 µM) were analyzed further at 5 µM increment, such that amount of honokiol

would be nonlethal but sufficient to suppress cell proliferation. The seeding concentration for BAEC was relatively high for the first round and the control reached confluency rapidly, therefore the experiment was terminated at day 4. From figure 10, it can be seen that growth-inhibitory effect of honokiol was delayed for two days after its addition to the growth medium. Although the inhibitory effect on BAEC was relatively steady after day 2, BSMC seemed to have the ability to overcome honokiol after day 4. Further experiments with extend length of study are required to confirm this finding and finer titration of honokiol concentration is needed to determine the exact inhibitory concentration. The morphological changes of cells due to honokiol were also noted. Higher concentrations of honokiol not only inhibited cell proliferation, but also significantly reduced the cell size. However, the underlying cell mechanism requires further investigations. In addition, this study was performed on bovine cells, which potentially react to honokiol differently from human cells. Therefore, this study needs to be repeated with human primary cells to confirm the drug efficacy. Although more in-depth research is necessary for consideration of honokiol for clinical usage, the current results show that it has the potential to be used in drug-eluting stents for angioplasty to prevent restenosis.

CHAPTER THREE

Application of the Live Cell Labeling Probe: In Vitro Thrombectomy Study

Introduction

Stroke is among the top five causes of death with over 100,000 incidences in the US every year [29]. Ischemic stroke is commonly caused by thrombosis, where the occlusion of the blood vessel limits the blood supply to the brain and leads to rapid brain damage. Anticoagulants are used at an early stage to limit the size of the clot, while thrombolytic drugs such as intravenous tissue plasminogen activator (tPA) are applied for more severe cases. For acute ischemic strokes, surgical intervention becomes necessary. Traditional clot removal through surgical incision has been replaced with catheter thrombectomy through aspiration or retrieval devices [30].

There are a number of FDA approved endovascular mechanical thrombectomy devices for treating ischemic stroke. Clinical trials have shown a 48% recanalization rate for the first generation Merci devices [31]. When coupled with adjunctive therapy such as tPA, second-generation Merci L5 retriever increased the recanalization rate to 69% with reduced mortality rate [32]. There have been studies on the clinical and angiographic outcomes of the patients, and complications during clot removal have been associated with systolic blood pressure [33]. Compared to the Merci devices, Solitaire and Penumbra achieved significantly higher recanalization rates of 90% and 93%, respectively, with their self-expanding and fully retrievable devices, and immediate blood flow restoration was observed for some patients upon device deployment [34, 35].

Although primary clinical outcomes have demonstrated these devices as a safe, rapid and effective method for retrieving clot within an 8-hour window of symptom onset,

in vivo studies in swine have indicated potential problems with these systems. Aspiration devices with a proximal approach have only a 40% success rate in retrieving the clot material [30]. Since basket-like distal retrieval devices physically trap the thrombus, they have a much higher success rate of 82% [30]. However, due to the compaction of the clot during distal retrieval, there is an increased risk for vessel wall injury, which would lead to a higher incidence of thromboembolic events and vasospasms [30].

An improvement in understanding of these potential complications can greatly increase the success rate of clinical trials, reduce the long-term cost and provide insight into the modification of device design. To systematically evaluate the impact of the mechanical thrombectomy devices on the endothelial lining of the vessel wall, we have developed a novel in vitro model consisting of a transparent silicon vessel seeded with endothelial cells. MitoTracker Red described in Chapter 1 is used to label cells for monitoring the thrombectomy process and analyzing the condition of vessel wall post-procedure.

Methods

PDSM Vessel Preparation

5% agarose solution was injected into a rubber mold to make rods with 3.5 mm in diameter. PDMS (made with silicone elastomer kit from Dow Corning Corporation) tubes were casted around the agarose rods by double coating the rods in PDMS solution and cured at 60 ℃ for one hour each time. The PDMS tubes were treated 30 min each with acetone, water boiling, heated 5M NaOH, plasma activation and 3% acetic acid. Sulfo-SANPAH (Bioworld) was chemically linked to the inside of the tubes by UV activation

twice at 365 nm, 8 min each time. After PBS wash, the tubes were coated with 344 μg/ml collagen (BD Scientific) at 4 ℃ overnight.

Cell seeding

BAECs were cultured to near confluency and seeded to 80% confluency inside the PDMS vessels, which were sterilized with UV. After the cell suspension was dispensed into the tubes, the PDMS vessels were incubated at 37 ℃ and rotated 90 ºevery 5 min for 30 min for even cell seeding, and cells were allowed to attach and spread for another 2 hours afterwards.

Bioreactor Assembly

The cells-seeded PDMS vessels were mounted onto rectangular PDMS chambers via connector tubes at each end and secured with elastic bands or sutures. The chambers with vessels were then sandwiched between two glass slides with a plastic connector on each side. Rubber tubes connected the vessels with a growth medium reservoir in a closed circulation system, which was connected to a pump to generate unidirectional flow in the system.

Thrombectomy Procedure

After the cells were exposed to flow for 24-72 hours, the circulating system was removed from the pump, and cells in the PDMS vessels were stained with 62.5 nM MitoTracker Red for 30 min. Swine blood clot was injected into the cell-seeded vessels and allowed to adhere for 15 min. The guide catheter (Penumbra) was inserted into the

rubber tubes and stopped just before the PDMS vessel. The delivery microcatheter (Penumbra) containing the collapsed retrieval device (Separator 3D, Penumbra or Trevo Pro Retrieval System, Concentric Medical) was inserted inside the guide catheter until the tip passed the clot. The delivery microcatheter was pulled back to release the self-expanding retrieval device. After the device was expanded and clot captured, with vacuum suction applied at the open end of the catheter, the retrieval device with the catheter was withdrawn to remove the clot from the vessel. The entire process was monitored live under a fluorescent microscope.

Results

The full circulation system with the bioreactor, three-way valve and pump is shown in figure 12A. Figure 12B illustrates the components of the bioreactor. The PDMS chamber that holds the cell-seeded PDMS vessels was sandwiched between two glass slides and secured with plastic connectors on the two sides (metal clips were used in figure 12A as connectors). The PDMS tubes were seeded with a confluent layer of BAEC and exposed to steady flow in the circulation system for 3 days before the introduction of blood clot, so that cells were spread out and aligned with the flow direction (figure 12D).

The BAEC-seeded vessels were stained with 62.5 nM MitoTracker Red before the thrombectomy procedure, which was monitored live under the microscope. The major steps are outlined in figure 13, and the corresponding locations indicated by the arrows are depicted in figure 14. Moderate amount of cell loss was observed after the introdution of the clot into the vessel (figure 14B). As the catheter slid along the cell sheet, a thin line of cells were scrapped off (figure 14C). After the retrieval device was deployed, cells

were pressed against the vessel wall by the wire of the device. Slight movements of the device caused cell detachment at the immediate impact region, while the rest of the cell sheet was still intact (figure 14D1, D2). During device withdrawal, large patches of cells were scrapped off by the wire (figure 14E1, E2). After the clot was completely removed by the device, significant cell loss was observed, with sharp edges of the remaining cell patches matching the shape of the wire.

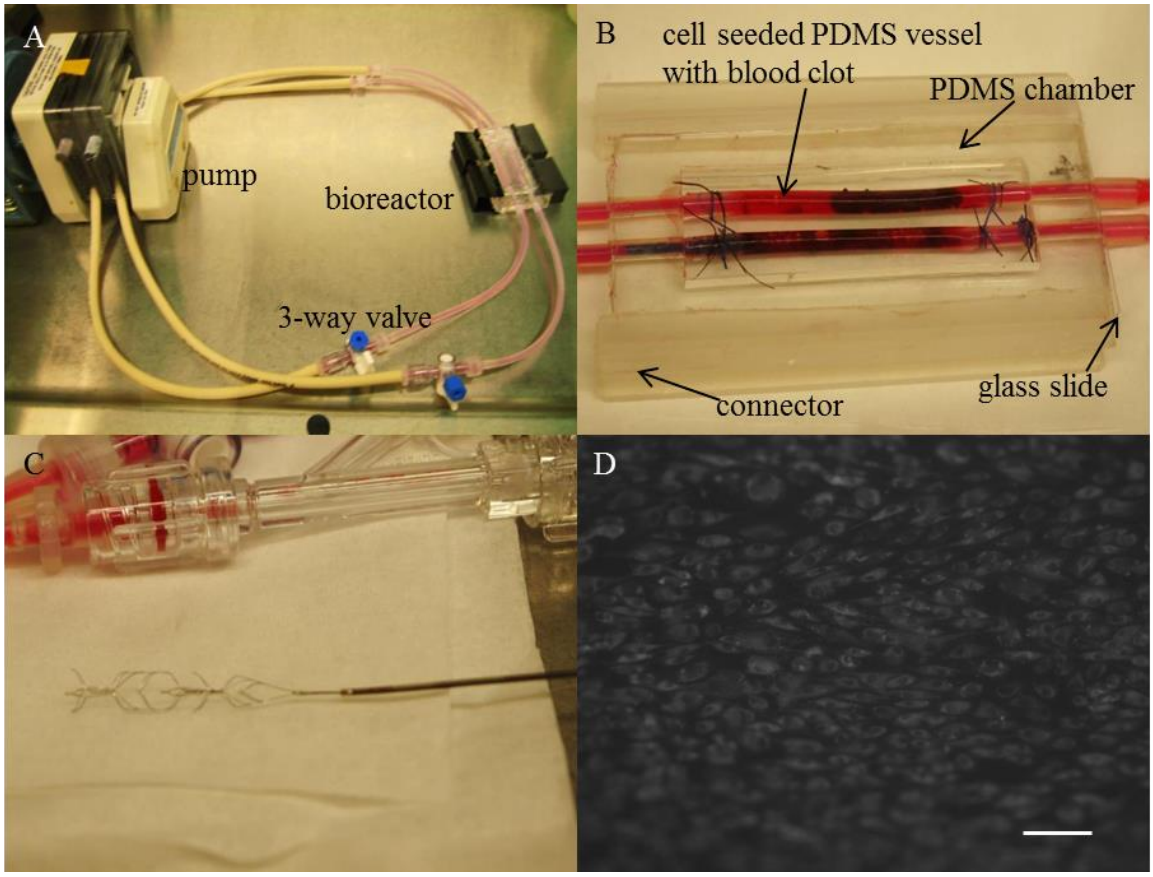

Figure 12. A: setup of the circulation system. B: components of the bioreactor. C: clot retrieval device Separator 3D from Penumbra. D: confluent BAEC sheet in the PDMS vessels under flow, stained with MitoTracker Red. Scale bar = 100 μm.

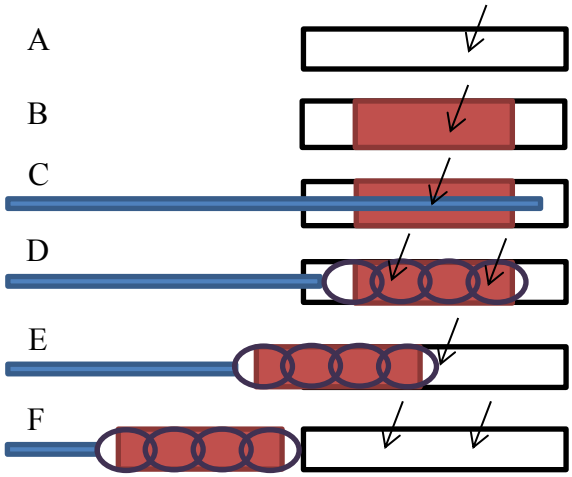

Figure 13. Outline of the thrombectomy procedure. A: cell-seeded PDMS vessel. B: blood clot introduced into the vessel. C: catheter guiding the retrieval device inside passed through the clot. D: catheter withdrawn to the end of the clot to deploy the device. E: device with clot trapped pulled back. F: device with clot completely withdrawn from the vessel.

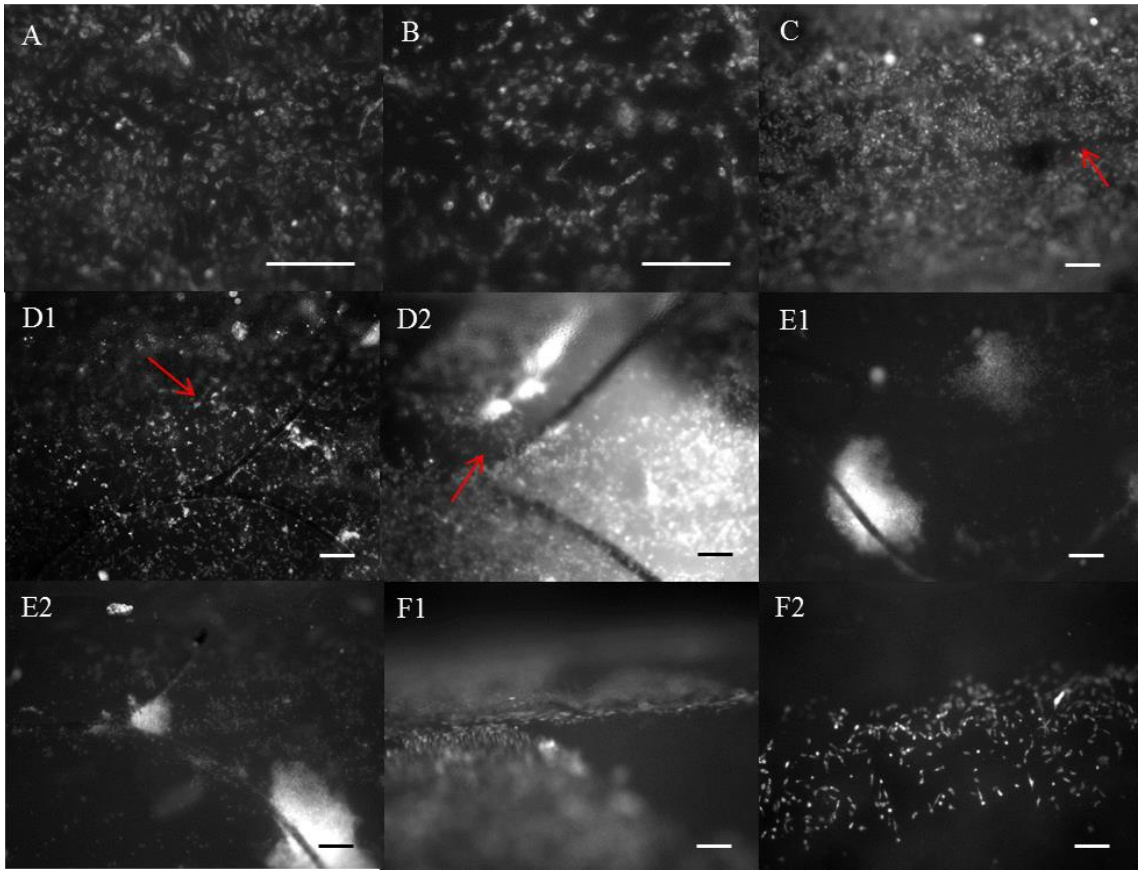

Figure 14. Conditions of cell sheet lining the PDMS vessels during thrombectomy using the Trevo Pro Retrieval System. Image locations correspond to the arrows in figure 13. Arrows point to damaged cell lining due to the catheter (C) and the wire on the retrieval device (D1, D2). Scale bar = 200 μm.

Discussion

In addition to long-term tracking, MitoTracker Red was also relatively resistant to photobleaching. Its prolonged signal strength after staining made it possible to perform live monitoring of the thrombectomy process.

With real-time recording, it was possible to identify the specific part of the retrieval device that did the most damage to the cell sheet. Although the cell attachment strength to the PDMS vessel in comparison to a native blood vessel was not evaluated, the cell sheet was strong enough to stay mostly intact after the clot introduction and device deployment, the only exception was the region that had direct contact with the catheter and the wire on the retrieval device. During the device withdrawal period, however, cells were scrapped off in large patches, especially at the tip of the device, which would likely happen when the procedure is performed with a real blood vessel.

One concern of the experiment was the limited incubation period with the clot in the vessel, which was probably not long enough for the clot to firmly adhere to the vessel, and hence a single execution of thrombectomy was sufficient to remove most of the clot. In pathological conditions where the clot is structurally integrated with the vessel, multiple operations would be required to fully extract the clot and hence more damage would be done to the endothelial lining of the vessel wall. Even without the full thrombectomy procedure, our preliminary results suggest possible improvements to the design of the retrieval device.

The next step would be a live video recording of thrombectomy with a modified bioreactor set up. New device design can be analyzed in this system to assess the degree of damage to the vascular endothelial layer. Drugs such as honokiol can also be

incorporated into the device, which can either promote endothelial cell recovery or inhibit smooth muscle cell growth to prevent rethrombosis. The efficacy of drug-coated retrieval device can also be evaluated with this in vitro vessel model and the long-term effect of the drug on the vessel lining can be studied.

CONCLUSIONS

Among the eight cell-labeling molecular probes tested, only MitoTracker Red was suitable for long-term live cell tracking under the experimental conditions. Although calcein AM generated excellent signals, it considerably inhibited cell growth even at 250 nM, which was a quarter of the lowest recommended working concentration. Even though the fluorescent signal produced by MitoTracker Red at 62.5 nM was less intense and it was also associated with relatively high background noise, it did not significantly interfere with cell proliferation over five days. The weak MitoTracker Red signal did not significantly affect image quality since the image analysis software, CellProfiler, was able to practically correct the background interference while enhancing the object signal. With parameters adjusted for each set of images, the cell count quantification process was automated with the object identification pipeline of CellProfiler. This experimental setup with MitoTracker Red for cell-labeling and CellProfiler for image processing is very useful for a number of applications, two of which were demonstrated.

One potential application for live cell tracking is drug screening. MitoTracker Red was used to track the effect of honokiol on BAEC and BSMC growth over an extended period of time. Since cells could be repeatedly stained with MitoTracker Red without growth interference, the cell proliferation under each drug condition could be followed throughout the course of the study without the need to terminate any experimental group at each time point. Preliminary findings suggested a growth inhibition concentration of honokiol for each cell type (55 μM for BAEC, 60 μM for BSMC). Although further research is required to finely titrate the inhibition concentration and assess the cellular

condition over a longer time period, this study demonstrated the potential of MitoTracker Red as a cell tracking reagent in drug testing.

MitoTracker Red was also used to monitor a thrombectomy procedure in real time, performed in a novel in vitro vessel model. With BAEC fluorescently labeled, the clot retrieval process inside the transparent cell-seeded PDMS vessels was captured live. It was observed that both the catheters and the retrieval devices caused damage to the endothelial cell sheet. In the case of the Trevo Pro Retrieval System, the most destruction was caused by the wire at the tip of the device when the clot was withdrawn into the catheter. In addition to assessing the immediate impact of the thrombectomy procedure to the vessel wall, the long-term consequences can be evaluated as well. This system is a robust platform for testing clot retrieval devices prior to costly and time-consuming in vivo studies and clinical trials. It can provide insightful suggestions for designing new devices or modifying the design of existing devices.

REFERENCES

1. Beutner, E.H., *Immunofluorescent staining: the fluorescent antibody method.* Bacteriological reviews, 1961. **25**(1): p. 49.

2. Tsien, R.Y., *The green fluorescent protein.* Annual review of biochemistry, 1998. **67**(1): p. 509-544.

3. Latt, S.A. and J.C. Wohlleb, *Optical studies of the interaction of 33258 Hoechst with DNA, chromatin, and metaphase chromosomes.* Chromosoma, 1975. **52**(4): p. 297-316.

4. Pjura, P.E., K. Grzeskowiak, and R.E. Dickerson, *Binding of Hoechst 33258 to the minor groove of B-DNA.* Journal of molecular biology, 1987. **197**(2): p. 257-271.

5. O'Brien, J., I. Wilson, T. Orton, and F. Pognan, *Investigation of the Alamar Blue (resazurin) fluorescent dye for the assessment of mammalian cell cytotoxicity.* European Journal of Biochemistry, 2000. **267**(17): p. 5421-5426.

6. Hamid, R., Y. Rotshteyn, L. Rabadi, R. Parikh, and P. Bullock, *Comparison of alamar blue and MTT assays for high through-put screening.* Toxicology in vitro: an international journal published in association with BIBRA, 2004. **18**(5): p. 703.

7. Presley, A.D., K.M. Fuller, and E.A. Arriaga, *MitoTracker Green labeling of mitochondrial proteins and their subsequent analysis by capillary electrophoresis with laser-induced fluorescence detection.* Journal of Chromatography B, 2003. **793**(1): p. 141-150.

8. Minamikawa, T., A. Sriratana, D.A. Williams, D.N. Bowser, J.S. Hill, and P. Nagley, *Chloromethyl-X-rosamine (MitoTracker Red) photosensitises mitochondria and induces apoptosis in intact human cells.* Journal of Cell Science, 1999. **112**(14): p. 2419-2430.

9. Pendergrass, W., N. Wolf, and M. Poot, *Efficacy of MitoTracker Green™ and CMXRosamine to measure changes in mitochondrial membrane potentials in living cells and tissues.* Cytometry Part A, 2004. **61**(2): p. 162-169.

10. Poot, M., L.L. Gibson, and V.L. Singer, *Detection of apoptosis in live cells by MitoTracker™ Red CMXRos and SYTO dye flow cytometry.* Cytometry, 1997. **27**(4): p. 358-364.

11. Chazotte, B., *Labeling lysosomes in live cells with LysoTracker.* Cold Spring Harbor Protocols, 2011. **2011**(2): p. pdb. prot5571.

12. Freundt, E.C., M. Czapiga, and M.J. Lenardo, *Photoconversion of Lysotracker Red to a green fluorescent molecule.* Cell research, 2007. **17**(11): p. 956-958.

13. Uggeri, J., R. Gatti, S. Belletti, R. Scandroglio, R. Corradini, B.M. Rotoli, and G. Orlandini, *Calcein-AM is a detector of intracellular oxidative activity.* Histochemistry and cell biology, 2000. **122**(5): p. 499-505.

14. Braut-Boucher, F., J. Pichon, P. Rat, M. Adolphe, M. Aubery, and J. Font, *A non-isotopic, highly sensitive, fluorimetric, cell-cell adhesion microplate assay using calcein AM-labeled lymphocytes.* Journal of immunological methods, 1995. **178**(1): p. 41-51.

15. Songa, E.-C., S.-J. Kima, D.-I. Sinna, J.-H. Kima, D.-K. Parka, K.-M. Kanga, N.H. Honga, H.-K. Parka, C.-H. Wonf, and K.-H. Kimf, *Systemic transplantation of human adipose stem cells attenuated cerebral inflammation and degeneration in a hemorrhagic stroke model.* 2007.

16. Zhang, W., A.L. McIntosh, H. Xu, D. Wu, T. Gruninger, B. Atshaves, J.S. Liu, and F. Schroeder, *Structural analysis of sterol distributions in the plasma membrane of living cells.* Biochemistry, 2005. **44**(8): p. 2864-2884.

17. Ko, C.-H., H.-H. Chen, Y.-R. Lin, and M.-H. Chan, *Inhibition of smooth muscle contraction by magnolol and honokiol in porcine trachea.* Planta medica, 2003. **69**(06): p. 532-536.

18. Fujita, M., H. Itokawa, and Y. Sashida, *Studies on the components of Magnolia obovata Thunb. 3. Occurrence of magnolol and hõnokiol in M. obovata and other allied plants].* Yakugaku zasshi: Journal of the Pharmaceutical Society of Japan, 1973. **93**(4): p. 429.

19. Bai, X., F. Cerimele, M. Ushio-Fukai, M. Waqas, P.M. Campbell, B. Govindarajan, C.J. Der, T. Battle, D.A. Frank, and K. Ye, *Honokiol, a small*

molecular weight natural product, inhibits angiogenesis in vitro and tumor growth in vivo. Journal of Biological Chemistry, 2003. **278**(37): p. 35501-35507.

20. Ishitsuka, K., T. Hideshima, M. Hamasaki, N. Raje, S. Kumar, H. Hideshima, N. Shiraishi, H. Yasui, A.M. Roccaro, and P. Richardson, *Honokiol overcomes conventional drug resistance in human multiple myeloma by induction of caspase-dependent and-independent apoptosis.* Blood, 2005. **106**(5): p. 1794-1800.

21. Wang, T., F. Chen, Z. Chen, Y.-F. Wu, X.-L. Xu, S. Zheng, and X. Hu, *Honokiol induces apoptosis through p53-independent pathway in human colorectal cell line RKO.* World Journal of Gastroenterology, 2004. **10**(15): p. 2205-2208.

22. Fried, L.E. and J.L. Arbiser, *Honokiol, a multifunctional antiangiogenic and antitumor agent.* Antioxidants & redox signaling, 2009. **11**(5): p. 1139-1148.

23. Ho, K.Y., C.C. Tsai, C.P. Chen, J.S. Huang, and C.C. Lin, *Antimicrobial activity of honokiol and magnolol isolated from Magnolia officinalis.* Phytotherapy Research, 2001. **15**(2): p. 139-141.

24. Chen, J.-H., C.-C. Wu, G. Hsiao, and M.-H. Yen, *Magnolol induces apoptosis in vascular smooth muscle.* Naunyn-Schmiedeberg's archives of pharmacology, 2003. **368**(2): p. 127-133.

25. Wu, C.-H., C.-W. Chen, H.-C. Chen, W.-C. Chang, M.-J. Shu, and J.-S. Hung, *Elucidating the inhibitory mechanisms of magnolol on rat smooth muscle cell proliferation.* Journal of pharmacological sciences, 2005. **99**(4): p. 392-399.

26. Lee, B., C.-H. Kim, and S.-K. Moon, *Honokiol causes the p21WAF1-mediated G (1)-phase arrest of the cell cycle through inducing p38 mitogen activated protein kinase in vascular smooth muscle cells.* FEBS letters, 2006. **580**(22): p. 5177.

27. Hu, H. and X.x. ZHANG, *Honokiol inhibits arterial thrombosis through endothelial cell protection and stimulation of prostacyclin.* Acta Pharmacologica Sinica, 2005. **26**(9): p. 1063-1068.

28. Wang, X., X. Duan, G. Yang, X. Zhang, L. Deng, H. Zheng, C. Deng, J. Wen, N. Wang, and C. Peng, *Honokiol crosses BBB and BCSFB, and inhibits brain tumor growth in rat 9L intracerebral gliosarcoma model and human U251 xenograft glioma model.* PLoS One, 2011. **6**(4): p. e18490.

29. Towfighi, A. and J.L. Saver, *Stroke Declines From Third to Fourth Leading Cause of Death in the United States Historical Perspective and Challenges Ahead.* Stroke, 2011. **42**(8): p. 2351-2355.

30. Gralla, J., G. Schroth, L. Remonda, K. Nedeltchev, J. Slotboom, and C. Brekenfeld, *Mechanical Thrombectomy for Acute Ischemic Stroke Thrombus–Device Interaction, Efficiency, and Complications In Vivo.* Stroke, 2006. **37**(12): p. 3019-3024.

31. Smith, W.S., G. Sung, J. Saver, R. Budzik, G. Duckwiler, D.S. Liebeskind, H.L. Lutsep, M.M. Rymer, R.T. Higashida, and S. Starkman, *Mechanical thrombectomy for acute ischemic stroke final results of the multi MERCI trial.* Stroke, 2008. **39**(4): p. 1205-1212.

32. Smith, W., *Safety of mechanical thrombectomy and intravenous tissue plasminogen activator in acute ischemic stroke. Results of the multi Mechanical Embolus Removal in Cerebral Ischemia (MERCI) trial, part I.* American Journal of Neuroradiology, 2006. **27**(6): p. 1177-1182.

33. Nogueira, R.G., D.S. Liebeskind, G. Sung, G. Duckwiler, and W.S. Smith, *Predictors of Good Clinical Outcomes, Mortality, and Successful Revascularization in Patients With Acute Ischemic Stroke Undergoing Thrombectomy Pooled Analysis of the Mechanical Embolus Removal in Cerebral Ischemia (MERCI) and Multi MERCI Trials.* Stroke, 2009. **40**(12): p. 3777-3783.

34. Castaño, C., L. Dorado, C. Guerrero, M. Millán, M. Gomis, N.P. de la Ossa, M. Castellanos, M.R. García, S. Domenech, and A. Dávalos, *Mechanical thrombectomy with the solitaire AB device in large artery occlusions of the anterior circulation A pilot study.* Stroke, 2010. **41**(8): p. 1836-1840.

35. Kulcsár, Z., C. Bonvin, V. Pereira, S. Altrichter, H. Yilmaz, K.-O. Lövblad, R. Sztajzel, and D.A. Rüfenacht, *Penumbra system: a novel mechanical thrombectomy device for large-vessel occlusions in acute stroke.* American Journal of Neuroradiology, 2010. **31**(4): p. 628-633.